Tectonic Control on the Pachmarhi Drainage System

Dr. N.L. Dongre

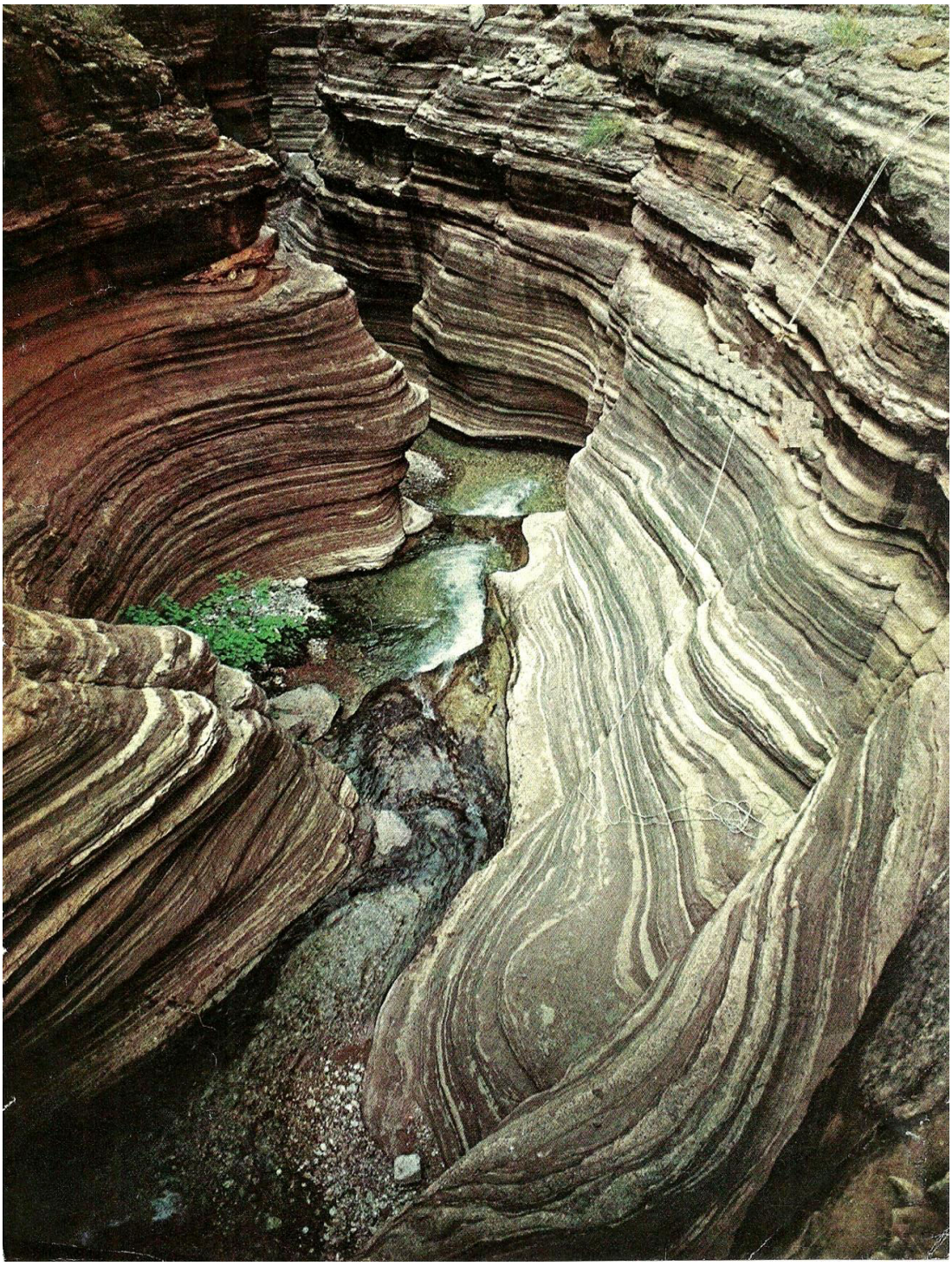

Marvellous scene of Denwa River drainage and tectonic uplift of Dhupgarh Mountain.

ABSTRACT: Drainage channels in the Pachmarhis are preferentially oriented parallel and perpendicular to the direction of tectonic extension. This pattern has been variably attributed to such causes as tectonic tilting during extension, channel elongation by slip along the

Ran ge -bounding detachment fault, and the exploitation of extension-rela ted joint sets during channel incision. In this paper I have used field observation, digital elevation, model analyses, and numerical modeling to test hypotheses for the tectonic control of Drainage system in the Pachmarhis, using the Pachmarhis as a type example. Field measurements and aerial photographic analyses indicate that channels of all sizes exploit steeply dipping joint sets during fluvial incision. As a consequence, channels become preferentially aligned along those joint sets. First and second Strahler-order channels preferentially exploit a joint set oriented perpendicular to the extension direction, while higher-order channels preferentially exploit a joint set oriented parallel to the extension direction. While these observations support the joint-exploitation hypothesis for structural control of drainage architecture, numerical modeling indicates that the spatial distribution of rock uplift during the initial phase of extension plays a crucial role by determining which joint set is preferentially exploited by channels of which Strahler orders. Numerical models indicate that higher-order channels exploit the joint set that is most closely aligned with the direction of initial tectonic tilting, even if that tilting is active for only a short period of time following the initiation of uplift. I conclude that the drainage architecture in the the Pachmarhis is the result of a combination of joint exploitation and tectonic tilting mechanisms. Structure also plays an important role in controlling the longitudinal profiles of channels in the Pachmarhis. Channels in the the Pachmarhis are characterized by structurally controlled knick points with a wide distribution of heights and spacings. Field observations indicate that the occurrence of structurally controlled knickpoints and the resulting variability in longitudinal profile form is related to spatial variations in joint density. Numerical models that incorporate spatial variations in joint density using a stochastic bedrock erodibilty coefficient are capable of reproducing the statistical properties of longitudinal profiles in the Pachmarhis, including the power spectrum of longitudinal profiles and the frequency size distribution of structurally controlled knickpoints. The results of this study illustrate the important roles played by both jointing and the spatial distribution of rock uplift on the geomorphic evolution of the Pachmarhis. More broadly, the study provides a recipe for how to incorporate joint-related structural controls into landscape evolution models.

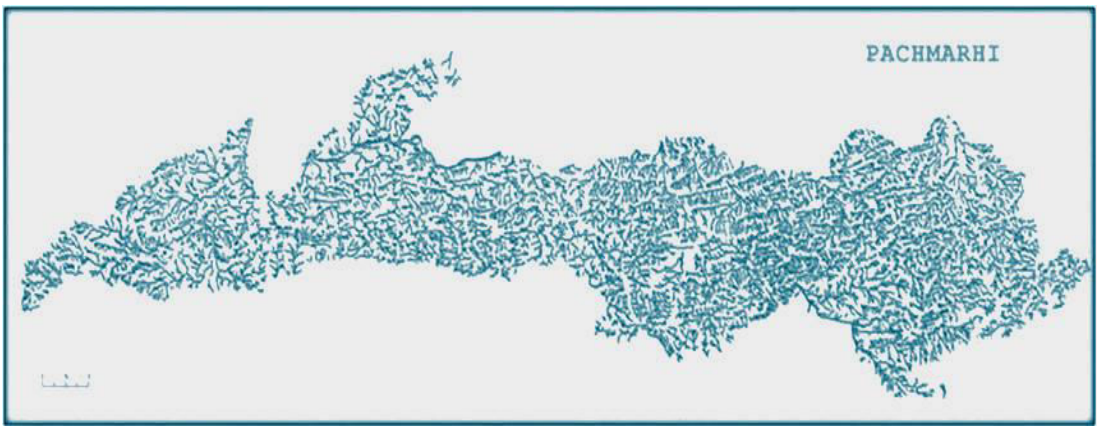

Figure: 1.Tectonically controlled drainage net work in the Pachmarhi

Introduction

A better understanding of the topographic evolution of mountain belts requires a better quantitative understanding of how bedrock channels behave. Early modeling work on

the evolution of bedrock channels emphasized the relationships between drainage area, uplift rate, and longitudinal profile form in relatively simple cases of uniform tectonic upliftrate and rock type (e.g., Whipple and Tucker, 1999). More recently, the impact of variations in tectonic uplift rate, sediment supply, and substrate heterogeneity on the morphology of bedrock channels has been emphasized (Finnegan et al., 2005; Wobus et al., 2006; Amos and Burbank, 2007; Gasparini et al., 2007; Pazzaglia et al., 2007; Turowski et al., 2007; Whittaker et al., 2007). Studies have shown that bedrock channels can respond to differential uplift or variations in substrate erodibility in complex ways. Channels adjust both in width and slope to variations in uplift rate or resistance to erosion. As a result, positive or negative feedbacks can occur between erosion rate, channel width, and channel slope (Amos and Burbank, 2007; Whittaker et al., 2007; Attal et al., 2008). Channels can also pass a threshold channel gradient beyond which a reduction in bed shear stress occurs in spite of the bed steepness (Crosby et al., 2007). In such cases, tectonically and structurally controlled knickpoints can persist in the landscape long after they are formed. In this paper,I focus on the role of substrate variability on the orientation and longitudinal profiles of bedrock and mixed bedrock-alluvial channels in a tectonically active, Pachmarhi and Mahadeva rock system of Satpura.

Topographically, the Pachmarhis form spatially discontinuous mountain ranges with relief of as much as 1400 meter and widths of ~20 km. Fluvial drainages in the Pachmarhis(Figure.1) are often aligned preferentially parallel and perpendicular to the extension direction. This apparent tectonic and structural control on drainage architecture has puzzled geologists for at so many years (Figure.2). Nevertheless, despite their prominence in the Pachmarhi landscape has been the focus of few geomorphologic studies. In this paper, I address three problems: (1) a classic problem in Mahadeva geomorphology (the origin of linear valleys aligned parallel to the extension direction), (Figure.-3).(2) problems of general relevance to geomorphology in a range of settings (joint control on network geometry and separately on profile shape), (Figure.-4) and (3) a methodological problem (simulating anisotropic erodibility on a regular grid).

I have noted locations, where initially extension-parallel drainages had been captured by radially oriented drainages. I used these observations to propose a two-stage model for the tectonic control of drainage architecture in the Pachmarhi(Figure.5). In the model, extension-parallel drainages first form on a gently sloping ramp of footwall rocks exposed by tectonic denudation. Extension in the Pachmarhi is commonly accompanied by orthogonal contraction and antiformalBelkhandhar and Brijlaldeo mountains arching, diverts some of the linear drainages into a radial patternwhile preserving the extension-parallel orientation of drainages uplifted on drainage of Dhupgarh,Mahadeva and Chauragarh,the major antiformal axes. In some other way, I observed that extension-parallel drainages in the Pachmarhisare not restricted to the major antiformal axes: as such, there must be some additional mechanism of Nagan, Gohara, Ganjakunwar, Shrijonth,Kummajhir, Silpali, and Machidharfor controlling drainage architecture. My argument is that this additional mechanism was the repeated incision of channel segments into the footwall ramp after slip along the range-bounding detachment fault. I think maintenance of hydraulic linkage during sequential fault-slip events will guide the lengthening stream downthe fault ramp as the ramp is uncovered, and stream incision formed a progressively lengthening, extension-parallel, linear drainage segment.In addition, a small extension-parallel grooves in the newly exposed fault surface could further guide channels along the extension direction. Spencer's (2000) has presented the model whichis problematic for three reasons. First, in the absence of structural control, channels generally align along the direction of water flow, i.e., the direction of steepest descent. The direction of steepest descent prior to fluvial dissection is determined by the spatial distribution of rock uplift (e.g. tilting) near the range front. That direction may or

Figure: 2.The tectonic and structurally controlled columnar relief formation, due to rock joints and denudation at Jambudip.

Figure: 3. Denwa Rift valley, a part of the rift system originated in two main series of fractures but separated by a prolonged period of intermittent continental uplift and regional plantation, associated with pronounced trough-faulting and block-faulting.

Figure: 4.During different cycles, lowlands and troughs were developed respectively on the less resistant rocks and in the down-faulted blocks, bordered by high-level residuals of former erosion surfaces.

Figure: 5.Sonbhadra, the Rift Zone and the high-level residuals were believed to represent a “late Jurassic peneplain ".

Figure: 6.The orientation of joints and other extension-related structural elements, are extended to-perpendicular directions.

may not be parallel to the extension direction. Second, Spencer's (2000) model assumes that the channel is incising both upstream and downstream from the range-bounding detachment fault. In general, however, range-bounding faults coincide with the transition from erosion

(upstream of the fault) to deposition (downstream of the fault). Variations in the ratio of water and sediment through time cause the transition from erosion to deposition to fluctuate, but it is not generally the case that the range-bounding fault is upstream from that transition, as Spencer's model assumes.

Third, the model of Spencer does not address the occurrence of extension-perpendicular drainages.Joint exploitation is an appealing hypothesis for preferred drainage orientations in the Pachmarhisbecause it is readily observed in the field and in aerial photographs, and because the structural control is continuously exerted as channels incise more deeply into bedrock, rather than being a relict of an earlier control localized in time (e.g. during an early period of tilting) or in space (e.g. at a channel crossing the detachment fault). Miksa (1993) documented a higher frequency of channels oriented both parallel and perpendicular to the extension direction compared to channels oriented in other directionsin study area. Lower-order channels are preferentially oriented perpendicular to the extension direction; higher-order channels are preferentially oriented parallel to the extension direction. Joint alignment parallel and perpendicular to the extension direction is a general feature of all of the well-studiedthe Pachmarhis Mahadeva. Extension-parallel and extension-perpendicular joints developed in the Pachmarhi ranges as tectonic denudation relieved the remnant stresses imposed on the rocks in Oligocene-early Miocene time. A close association between the orientation of joints and other extension-related structural elements (e.g., fracture zones, dykes) and either the extension-parallel or extension-perpendicular directions was documented by Crookshank,H.(1936) in the Mahadeva. (Figure.6) The structural details of these ranges are, of course, complex and unique, but in all cases there are structural elements that provide extension-parallel and extension-perpendicular zones of weakness or heterogeneity that channels can exploit as they incise. Due to the general correlation between structural elements and extension-parallelor extension-perpendicular directions in the Pachmarhi of the Satpura,in my opinion a mechanism for the structural control of drainage orientation that could be broadly applicable to the Pachmarhi. (Figure.7) It is unclear whether joint control is the sole mechanismfor controlling drainage orientation in the Pachmarhi, or whether joint exploitation acts in concert with some other mechanism. it is also unclear why lower Strahler-order channels preferentially exploit the extension-perpendicular joint set while higher Strahler-order channels preferentially exploit the extension-parallel joint set.Figure.1 illustrates four areas with preferentially extension-parallel and extension-perpendicular drainages from the southern Pachmarhi. The extension direction is oriented west-southwest or approximately along a 240° azimuth. Of the four areas illustrated in the study,threeare considered the classic Pachmarhi-Dupgarh-Mahadeva-Chauragarh mountains, Tamia Patalkot scarpment and Denwa Sonbhadra rift valley.Higher-order drainages in the Pachmarhis are predominantly oriented parallel to the extension direction; lower-order drainages are oriented perpendicular to the extension direction. The Chauragarh Mountains exhibit the extension-parallel and extension-perpendicular drainage architecture as the other examples, but higher-order drainages are preferentially oriented perpendicular to the extension direction along a south-southeast-north-northwest orientation. The extension-perpendicular drainages in the Dhupgarh Mountains can be explained by north-northwest-striking normal faults, but the extension-parallel drainages in this range are not well understood.

North-draining channels are primarily oriented along the south-east-east-north-west extension direction. An alternative numerical model, which includes both joint exploitation and an early phase of extension-parallel tilting, is found to reproduce the observed drainage orientation patterns in the Pachmarhi In this model, the early phase of tilting causes higher-order drainages to exploit the joint set parallel to the extension direction. Lower-order drainages exploit the orthogonal, extension-perpendicular joint set, thus leading to drainage patterns similar to those observed in the Pachmarhis. Numerical modeling also suggests that Spencer's mechanism of channel orientation by slip along the detachment fault is not a viable mechanism for creating extension-parallel drainages.

Figure:7. Bainganga a very narrow stream, which has deeply incised the basalt rocks of the fault zone. mechanism for the structural control of drainage orientation that could be broadly applicable to the Pachmarhi. It is clear that joint control is the sole mechanism for controlling drainage orientation of the Pachmarhi.

I conclude that a combination of tectonic tilting model and joint-controlled model best explains the observed drainage architecture of the Pachmarhi. The numerical modeling discussion also explores an important, related feature of fluvial channels in the Pachmarhi i.e., their complex, stepwiselongitudinal profiles. Longitudinal profiles exhibit structurally controlled knickpoints and alternating zones of convexity and concavity over a wide range of

spatial scales. In the numerical modeling discussion I show how large-scale (i.e., 1-10 km) structurally controlled channel segments can result from small-scale (i.e., 1-10 m) variations in joint density and hence bedrock erodibility. The model I propose is capable of reproducing the statistical properties of actual longitudinal profiles from with respect to both their power spectra and the frequency size distribution of structurally controlled kickpoints. In addition to exploring the controls of joint orientation and anisotropic density on the geomorphology of the Pachmarhis, this paper also provides a recipe for quantifying the role of anisotropic rock strength in landform evolution models more generally. Given the frequent occurrence of jointed bedrock in nature, the methods of this paper should provide a useful starting point for modeling structural controls on bedrock channel morphology in a broad range of other tectonic settings.

In this study I have used field measurements, digital elevation model (DEM) and areal photographic analysis and numerical modeling to test hypothesis for the tectonic control of drainage in the Pachmarhi.To plot the longtitudinal profiles of two representative channels of the Pachmarhi, the profiles were extracted from 1m/pixels light detection and ranging (LIDR) programme.

Numerical modeling

Three-Dimensional Model with Orientation-Dependent Bedrock Erodibility

The numerical models of this paper are based on the stream-power model of bedrock erosion, which in its basic form can be written as:

$$\frac{\partial h}{\partial t} = U - KA^m \left|\frac{\partial h}{\partial x}\right|^n, \quad (1)$$

Where*h*is elevation, *t*is time, *U* is the rock uplift rate, *K* is the coefficient of bedrock erodibility, *A* is the contributing area, *x* is the along-channel distance, and *m* and *n* are empirical coefficients (Whipple and Tucker, 1999). The stream-power model is most applicable to bedrock channels dominated by plucking, because it is in those channels where erosion rates can be related most directly with contributing area, a proxy for peak discharge (Whipple et al., 2000). In addition to the stream-power model, bedrock landform evolution models often include a hillslope erosion component. In this paper we do not include a hillslope erosion component because the pixel sizes of the model (100 m) are larger than the average distance between divides and channel heads in the study area. As such, bedrock channel erosion is the dominant process in the model down to the scale of individual pixels. The contributing area *A* in the model is calculated at each time step using the multiple-flow-direction method of Freeman (1991). This algorithm is implemented by first ranking all pixels in the basin from highest to lowest in elevation. Starting with the highest grid point in the basin, which receives only local runoff, flow is distributed to all of the neighbouring downslope pixels, weighed by slope.Routing is next performed for the second-highest grid point in the basin, then proceeding in rank order down to the lowest grid point. This method ensures that all incoming flow has been accounted for before the flow is distributed downstream.

Joint exploitation is included in the model by prescribing the bedrock erodibility,*K*, to be a function of channel orientation:

$$\frac{\partial h}{\partial t} = U - K(\theta - \varphi)A^m \left|\frac{\partial h}{\partial x}\right|^n, \quad (2)$$

where

$$K(\theta - \varphi) = K_0\{1 - \varepsilon_1 cos^2[\theta - \varphi]cos^2[\theta - (\varphi - \pi/2)] - \varepsilon_1 cos^2|\theta - \varphi|\}, \quad (3)$$

andK_0 is the maximum erodibility value, ε_1 and ε_2 are parameters that control the magnitude of the anisotropy, θ and φ are the local channel orientation and strike of the primary joint set, respectively. Equation 3 is a two-parameter function that mimics the form of the rose diagram of joint frequencies observed in the Pachmarhi. Equation 3 In this area, the drainages maintain their alignment with the local joint sets, not the regional extension directionalso assumes that the principal and secondary joint sets are orthogonal. If they are not, a second joint orientation can be introduced into equation 3 in place of the term $\varphi - \pi/2$ in order to represent the secondary joint set. The parameter ε_1 controls the strength of the anisotropy in K between channels aligned parallel to the primary and secondary joint sets and those not aligned parallel to these joint sets. Specifically, the ratio of the maximum to the minimum erodibility is given by $1/\varepsilon_1$. The parameter ε_2 controls the magnitude of the difference between the erodibility values for channels aligned along the primary versus secondary joint sets. For example, a value of $\varepsilon_2 = 0.5$ means that the bedrock erodibility coefficient along the secondary joint set is equal to half its value along the primary joint set. As an example, the diagram in (Figure 9B) plots the orientation dependence of K for $\varepsilon_1 = 2.5$, $\varepsilon_2 = 0$. As a caveat, equation 3 is only one possible approach to incorporating the effects of joints into bedrock-channel landscape evolution models. A more sophisticated model that explicitly incorporates data on joint spacing, length, and continuity would likely be the most ideal approach to this problem. Nevertheless, in this study I adopted a more empirical approach, effectively linking joint frequencies directly to bedrock erodibility values.

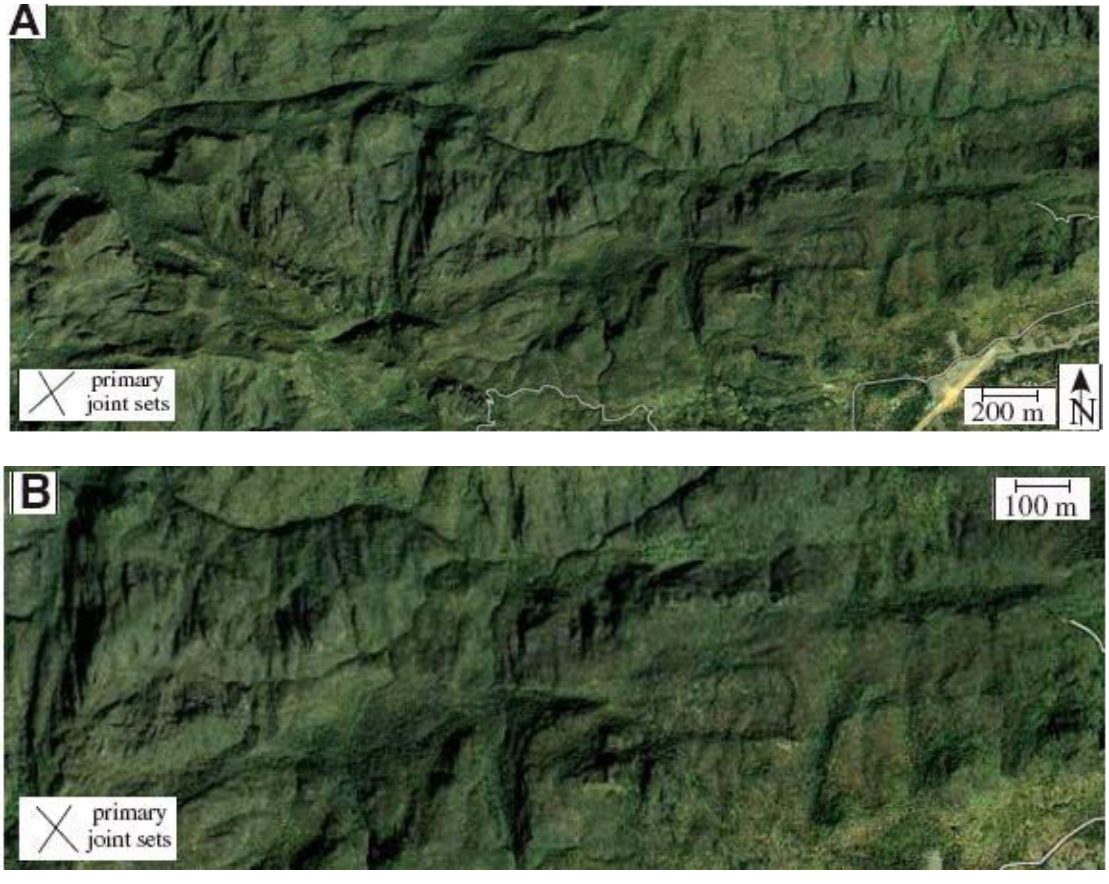

Figure: 8.Aerial photographs illustrating, examples of the correlation between joint and orientations locally. In each image, primary joints sets were identified by measuring the orientations of bedrock fractures visible in the photographs. This approach assumes that weathering and slope failure take place preferentially along joint sets, a hypothesis that is strongly supported by field observations. River lines highlight the locations where the local channel orientation closely aligns with one of the two primary joint sets. (A, B) The orientation of the primary joint sets is within 15° of the regionally averaged joint orientations, which, in turn, closely match with the extension-parallel and extension-perpendicular directions. (C) The primary joint sets are displaced ~45° counterclockwise from the regionally averaged orientations. (D) Part of toposheet 55J/7 depicting the Jambudip River and steep slop structure.

Introducing orientation dependence into a landscape evolution model raises a problem with regard to the underlying grid structure of the model. In landscape evolution models that operate on square pixels, the local channel slope and orientation are usually computed using the eight nearest neighbours to each pixel (including diagonals). This becomes problematic, however, when introducing anorientation dependence into K because channel orientations computed in this way are restricted to multiples of 45°. This fundamental discreteness resulting from a regular grid can be mitigated in two ways. First, the channel orientation and slope can be computed at a larger spatial scale using neighbours separated by one or more pixels between them (i.e., next-nearest neighbours or next- to next-nearest neighbours). Alternatively, the $D\infty$algorithm can be used (Tarboton, 1997). The $D\infty$algorithm identifies the two adjacent pixels amongst the nearest neighbours that have the lowest elevations. The elevations of those two pixels are then used to identify a channel orientation that can take on any continuous value between these two lowest adjacent neighbours. In the model of this paper,Ihave used the first method by calculating the channel slope and orientation using the next-nearest neighbours.This approach reduces, but does not eliminate the discreteness in channel orientation computed by the model. For the purposes of this paper, however, this method was found to work well.

The results of three model experiments designed to illustrate the effects of orientation-dependent bedrock erodibility are shown in (Figure. 9). Model results are shown for $U = 1\ m/ka$, K = 10^{-2} ka^{-1}, m = 0.5, n = 1, L = 40 km, and Δx = 100 m, where L is the

width and length of the domain and Δx is the pixel size. At the beginning of each model, the initial topography is a flat surface at $h = 0$ with a white noise of 1 m root-mean-squared amplitude superimposed. This white noise provides small-scale variations in flow pathways that represent the small-scale variations in topography orerodibility present in any area subject to incipient uplift. Each of the model experiments in this paper was run for 2 Ma. This duration was found to be sufficient for channel incision to propagate from the range front to the headwaters of the model domain near the center of the grid. Slope-area relationships for bedrock rivers indicate that $m/n \sim 0.5$ (Whipple and Tucker, 1999; Snyder et al., 2000). Here we choose the linear case of the stream power model (resulting in $m = 0.5$ and $n = 1$), but I verified that similar results were obtained for both linear and nonlinear model experiments. The values of U and K in the model control the elevation attained by the model for a given duration (i.e., higher values of K for a given U and model duration result in lower peak elevations). The values used in these experiments resulted in topography with a maximum elevation of ~2 km above base level, which is comparable to the relief of Pachmarhi. The value of U can be increased or decreased, and the resulting model topography is essentially unaffected. Only the time required to propagate knick points is affected by the absolute value of U as long as the ratio of U and K remains constant.

In the control case with $\varepsilon_1 = 0$ and $\varepsilon_2 = 0$, illustrated in (Figure 9A,) the drainages exhibit no structural control. The topography illustrated in (Figure 9A) is qualitatively similar to the output of stream-power-based landscape evolution models that have been described in the literature since the early 1990s (e.g., Willgoose et al., 1991; Howard, 1994). In contrast, (Figure.9B) illustrates the results of the model with $\varepsilon_1 = 2.5$, $\varepsilon_2 = 0$, and $\varphi = 240°$. These model parameters correspond to two equally erosive joint sets oriented at $\varphi = 240°$ (south-south-east-northeast) and $\varphi = 150°$ (south-southeast-north-northwest). (Figure.9B) clearly shows that channels tend to become aligned along the directions of peak erodibility values (which represent joint sets in the model). It is also apparent from (Figure.9B) that the choice of which joint set a particular set of channels exploits also depends on the channel orientation as established by the spatial pattern of uplift and/or the shape of the model domain. For channels draining to the bottom and top of the model domain, for example, the lower-order channels are predominantly aligned along the west-southwest-east-northeast joint set while the high-order channels are predominantly aligned along the south-southeast-north-northwest joint set. In the higher-order channels draining the Pachmarhi, the majority are aligned along the west-southwest direction, not the south-southeast direction. I conclude that joint control alone is insufficient to produce the drainage architecture observed in the Pachmarhi. Increasing or decreasing the value of ε_1 in the model increases or decreases the apparent structural control somewhat, but does not change the results qualitatively.

In addition to the anisotropy in bedrock erodibility caused by preferential joint orientations, there is another, more subtle, geomorphically relevant anisotropy that develops in Pachmarhi Dhupgar-Mahadeva-Chauragarh complexes. As described in the previous section, mylonitic rocks are composed of alternating bands (i.e., sills and the country rock into which they intrude) that strike along the extension direction. If joint densities differ between bands and folding occurs, elongated zones of relatively high and low joint densities aligned parallel to the extension direction are exposed in plan-form. This joint-density effect is separate from, but complimentary to, the joint-orientation effect represented in equation 3. This effect is likely enhanced by the presence of corrugations. Corrugations are large-scale folds (wavelengths of kilometers to tens of kilometers) that develop during exhumation. If the folding occurs late in exhumation, it can promote extension-parallel drainages via the tectonic effect of antiformalarching. Folding also causes additional structural effects in which mylonitic bands (i.e., laterally continuous zones of similar joint density) become exposed in planform, where they can be more readily exploited by incising channels. In the absence of corrugations, rivers will erode vertically through strong and weak bands, and this effect will likely be less significant in terms of generating preferential drainage orientations.


A
5 km
$\varepsilon_1 = 0, \varepsilon_2 = 0$


B
0.0 1.0 2.0 km
$\varepsilon_1 = 2.5, \varepsilon_2 = 0$


C
stochastic model for $K(x,y)$


D

Figure: 9.Grayscale maps of the topography predicted by the three-dimensional landscape evolution model based on the stream-power model for bedrock channel erosion, illustrating the role of orientation-dependent and spatially dependent bedrock erodibility on drainage architecture are also shown). The model domain is $40 \times 40\ km$ with a resolution of 100 m/pixel. In each case, rock uplift occurs at a rate of U = 1 m/ka for a duration of 2 Ma. (A) In the control model run, the parameters characterizing structural control, ε_1 and ε_2, were both set to zero. (B) The values were changed to $\varepsilon_1 = 2.5$ and $\varepsilon_2 = 0$, representing the effects of two equal joint sets oriented at $240°$ and 150°. (C) Grayscale map of the random erodibility co-efficient (with spatial correlations included in the extension-parallel direction). (D) Grayscale map of the toposheet 55/J 7,the model output using the *K(x, y)* map illustrated in C. In B and D, higher-order channels tend to be aligned along the joint set that is closest to the direction of uplift relative to base level (i.e., south-draining channels become aligned along the south-southeast-north-northwest direction, not along the west-southwest-east-northeast direction. (E) Part of the toposheet 55J/7, which explains the drainage pattern of the Bainganga River in the Pachmarhi.

In order to model this effect, I created a random noise for K with a mean value of 10^{-2} ka^{-1} uniformly distributed between $0.5 \times 10 - 2\ ka - 1$ and 2×10^{-2} ka^{-1} with spatial correlations in the extension-parallel direction and no correlations in the extension-perpendicular direction (Figure.9C). This random field was then input into the stream-power model, which produced the output shown in (Figure. 9D). As in the model output illustrated in Figure 9B, higher-order, south-draining channels tend to become aligned along the south-southeast-north-northwest-directed joint set, not the west-southwest-east-northeast joint set, as observed in the Pachmarhi(Figure.9E). As such, this effect does not appear to be sufficient to reproduce the drainage patterns observed in the Pachmarhi. The degree of anisotropy produced by this model depends on the standard deviation of K prescribed when generating the random noise; greater variation in K causes more anisotropy. One way to identify this effect separately from the joint-orientation effect represented by equation 3 is to note that bedrock erodibility is a function of channel orientation and strike direction, i.e., $K(\theta, \varphi)$, in equation 3 while in the case of Figures.9Cand Figure.9D it a function of space, i.e., K(x, y) and the channel orientation plays no explicit role. It is unclear how to distinguish these two joint-controlled using the topography or field observations alone, hence more research is needed. In the subsequent model experiments, I include the effects of joining using equation 3 only; bearing in mind that joint control can be exerted in two different ways.

Figures 10B and Figure.10D illustrate the results of two numerical experiments designed to test the tectonically driven hypotheses of Spencer (2000) and Pain (1985), respectively. Both model results use the same model parameters and forcing as Figure.9A,

except where noted. To test Spencer's hypothesis, I imposed spatially uniform uplift on the range, as in the control experiment of Figure. 9A, but I simultaneously extended the portion of the model domain subjected to uplift along a south eastward direction over time, as illustrated schematically in Figure.10A. Clearly, spatially uniform uplift is a simplification that is rarely, if ever, achieved in nature, and it is unlikely to be appropriate for the Pachmarhi. Nevertheless, it is useful to consider simplified end-member scenarios in order to isolate the effects of specific end-member mechanisms (e.g., mountain-front elongation versus tectonic tilting). Joint-controlled erosion with $\varepsilon_1 = 2.5$ and $\varepsilon_2 = 0$ was also incorporated in this model, as in Figure.9B. The results for this model scenario are shown in Figure 10B as a grayscale map of the topography at the end of the simulation *(t* = 2 Ma). The model results clearly illustrate that channels do not align in the extension-parallel direction. Instead, the model develops drainages that are perpendicular to the mountain front (i.e., south and east). This was also verified by performing numerical experiments with other mountain-front geometries; drainage networks develop perpendicular to the mountain front in all cases. In contrast, most of the higher-order drainages of The Pachmarhis are oriented along a west-southwest-east-northeast direction even though the mountain front is oriented in a west-northwest-east-southeast direction. The results of this numerical experiment indicate that elongation of the mountain front does not, as a general rule, create a preferred drainage orientation parallel to the direction of elongation or extension.

In the second tectonically driven model scenario, designed to test the hypothesis of Pain (1985), the model domain was first subjected to a short (i.e., 0.2 Ma) interval of tilting down to the west-southwest (240° azimuth). Following the initial phase of tilt-style uplift, a second, longer (1.8 Ma) interval of antiformal arching was imposed on the model domain with the arch axis following the same west-southwest-east-northeast Orientation as the initial tilting. In nature, extension and anti-formal arching in the Pachmarhis are essentially coeval. In these numerical experiments, however, we separated extension-parallel tilting and antiformal arching into two separate phases in order to simplify the experiments, and because, in nature, extension-parallel tilting most likely dominates the pattern of rock uplift. Contour maps of uplift rates for this model scenario are illustrated in Figure.10C. Orientation-dependent bedrock erodibility was also included in this model scenario to model the effect of Pain's model in combination with joint-controlled erosion. The results of this model, illustrated as a grayscale map of topography in Figure.10D, shows that drainages align parallel to the direction of initial tilting despite the fact that that tilting is only active for a small fraction (0.1 or 10%) of the model duration. The results of this model suggest that the initial spatial distribution of uplift plays an important role in controlling the subsequent drainage architecture because it is during this initial phase of rock uplift that incised channels become a permanent part of the landscape. Subsequent (or coeval) anti-formal arching causes some degree of channel reorganization into a radial pattern, but the extent of that reorganization is not sufficient to counteract the effect of the initial tilt-style uplift. I experimented with varying the duration of the initial phase of tilt-style uplift in the model by varying the duration of the initial tilt phase from just a few percent of the total model duration to as much as 50%. I found that as the duration of the initialtilt phase falls below 10% of the model duration (i.e., 200 m maximum relief generation given maximum uplift rates of *U* = 1 m/ka), the effects of initial tilting become less significant relative to the effects of subsequent anti-formal arching. As such, the initial phase of tilting must be sufficiently long to cause channels to incise to some minimum depth, below which they can be reoriented by a subsequent change in the spatial distribution of uplift. Once incision takes place beyond that minimum depth, however, the model results suggest that it is difficult for subsequent tectonic adjustments to substantially reorganize the drainage pattern.

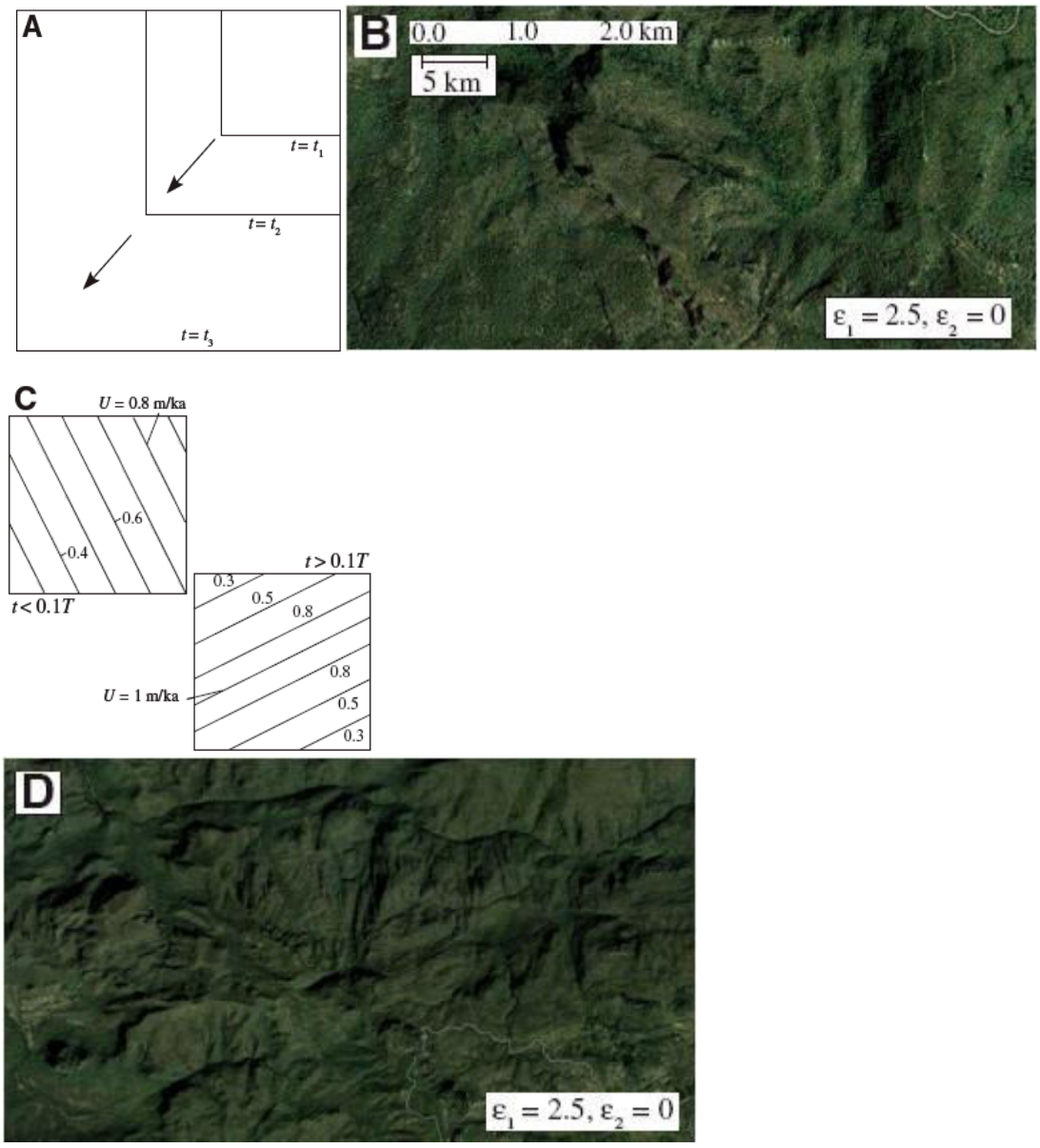

Figure: 10. Results of models designed to test the tectonic models of Spencer (2000) and Pain (1985) for extension-parallel drainage architectures in the Pachmarhis. (A) Imodeled the geomorphic response to spatially uniform uplift of a square model domain. The size of the square increases through time by domain extension in a southwestern direction. (B) The model result, shown as a grayscale map of topography, illustrates that this model produces parallel drainages oriented south and east, not southwest as predictedand prescribed by Spencer(2000). (C) Schematic illustration of the two-stage tectonic model proposed by Pain (1985). In this model scenario, tectonic tilting oriented in the south and south east direction takes place for the first 200 ka of a 2 Ma simulation. In the second stage of the model, antiformal arching takes place along an axis oriented in the southand south east direction (contour maps of uplift shown in C). T—duration of the simulation. (D) The model result shows higher-order channels oriented preferentially along the direction of the initial tilting and first-lower-order channels oriented preferentially along the south-southeast-north-northwest joint set. These results suggest that the initial spatial distribution of rock uplift exerts a first-order control on drainage architecture.

Figure 11 illustrates the results of applying the different structural and tectonic model scenarios to a model domain equal in size and shape to the actual Pachmarhi Mountains. It is useful to consider the model predictions in a domain similar to that of the study area because the results can then be more directly compared to the modern topography of the Pachmarhi (shown in Figure. 11A using the same scale as the model results in Figures. 11B) and 11D)

and because the shape of the boundaries of landscape evolution models can, in some cases, control the model results in complex and unexpected ways. The 1100m contour was chosen as the domain boundary for these models based on the fact that this elevation closely approximates the bedrock-alluvial contact at the mountain front of the actual Pachmarhi Mountains. However, is only an approximation to the actual location of the mountain front, because the mountain front does not follow contour precisely. (Figure.11B) illustrates the results of the model with joint controlonly (assuming $\varepsilon_1 = 2.5$, $\varepsilon_2 = 0$, and φ =240°). In these figures, the actual basin topography is shown for elevations below 1100 m (i.e., downstream from the base-level boundary condition imposed in the model).

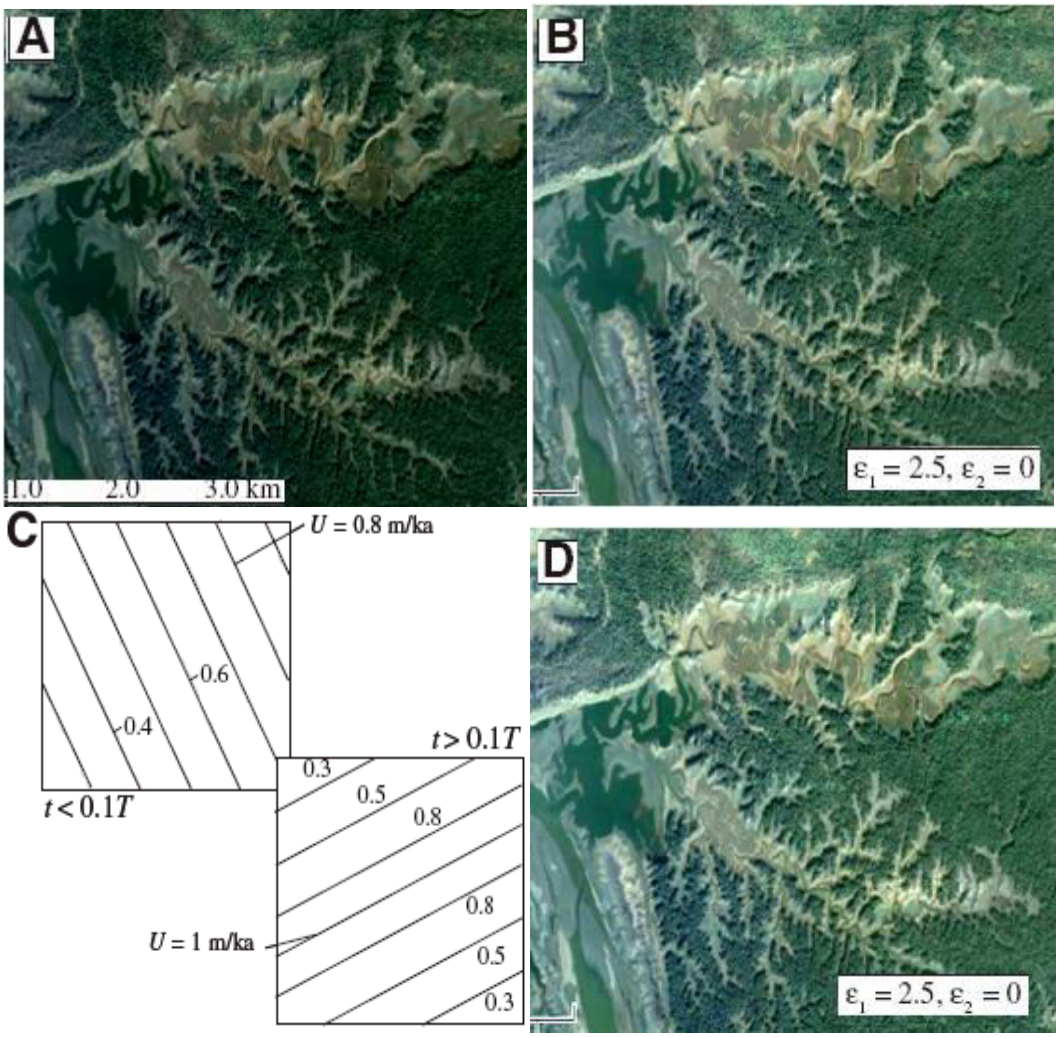

Figure 11.Results of models combining the structural and tectonic controls of Miksa (1993) and Pain (1985) and applied to a model domain matching the shape and extent of the Dhupgarh, Mahadevaand, Chauragarh Mountains. (A) Grayscale map of the actual topography of the Mountains. (B) Result of the model with orientation-dependent bedrock erodibilty($\varepsilon_1 = 2.5$ and $\varepsilon_2 = 0$) in which the domain was uplifted uniformly at U = 1 m/ka. (C) Two-phase model of tectonic tilting and antiformal arching. T-duration of the simulation. (D) The model with ($\varepsilon_1 = 2.5$ and $\varepsilon_2 = 0$)was used, but the domain was uplifted according to model shown schematically in C.

upliftis assumed to be spatially uniform in this model scenario. The results of the model are qualitatively similar to those ofthe same model performed on a square model domain (Fig. 9B). That is, in the area of the Pachmarhi, higher-order channels are preferentially oriented along the south-southeast-north-northwest joint set while lower-order channels are preferentially oriented along the orthogonal west-southwest-east-northeast joint set. In Figure 11D, the effects of joint-controlled incision are combined with the tectonic model of Pain (1985),

illustrated schematically in Figure 11C. Higher-order channels draining the southern and western flanks of the range are more preferentially aligned along the observed extension direction in this case as a result of the additional effect of the initial phase of tectonic tilting (not present in the model of Fig. 11B). Low-order channels in the model are preferentially oriented along the south-southeast-north-northwest joint set, illustrated in Figure 7C.

The model results illustrated in Figure 11 greatly simplify the tectonic, structural, and geomorphic processes of the range and do not represent a comprehensive model for the evolution of the Pachmarhi Mountains. For example, the topography of the Pachmarhi Mountains is controlled by high-angle faulting that are difficult to determine and that we have not attempted to include in the model. Despite the model simplifications, however, the results illustrated in Figures 9-11strongly support the conclusion that drainages are oriented parallel and perpendicular to the extension direction in the Pachmarhis due to a combination of joint-controlled bedrock channel erosion and an early phase of tectonic tilting that imposed an extension-parallel drainage architecture on the higher-order channels draining the southern flank of this metamorphic core complex.

Two-dimensional model with random spatial variations in erodibility

Field observations indicate that knickpoints in the Pachmarhi are controlled by spatial variations in bedrock erodibility related principally to local variations in joint density. Field observations indicate that kickpoint formation tends to be associated with the exposure of unusually thick (e.g., 1-3 m) leucogranite sills. It is these sills or light-toned bands that tend to have the lowest joint density and hence can be expected to have the lowest bedrock erodibility or *K* values. When incising channels encounter these bands, the channel must steepen locally relative to nearby channel segments in order to maintain comparable erosion rates along the longitudinal profile. Local channel steepening is required to maintain uniform erosion rates because higher values of stream power are required to pluck the larger blocks associated with channel segments of low joint density compared to nearby channel segments of higher joint density. If the local joint density falls below a certain threshold value, the channel may also be forced to erode by saltation abrasion, a process that is less efficient than plucking in the field, evidence for channel erosion

In this subsection I explore this conceptual model for the formation of structurally controlled longitudinal profile development using a simple mathematical model that treats bedrock erodibility as a random variable. The purpose of this model is not to predict precisely where kickpoints will occur in a given study area, but rather to understand the statistical properties of variations in longitudinal profile form. The longitudinal compositprofiles of channels in the Pachmarhi all exhibit variations over a wide range of scales (Figure. 12C). Despite this apparent complexity in form, the statistical properties of structurally controlled longitudinal profiles in the Pachmarhi show remarkable similarities that point to a common underlying mechanism for structural control in these channels. The stream power model with spatially variable erodibility can be written as:

$$\frac{\partial h}{\partial t} = U - K(x)A^{1/2}\left|\frac{\partial h}{\partial x}\right|, \qquad (4)$$

Using$m$ = 0.5 and n = 1. In this model, I represent spatial variations in joint density and the effect of those variations on erodibility using a stochastic model for *K(x).* In this model, *K(x)* is a random variable with values sampled at a prescribed interval Ax along the channel from a prescribed probability density function (pdf) with minimum and maximum values $K_{\min} and\, K_{\max,}$ respectively. For example, $k(x) = k_0$ for $o < x \leq \Delta x, K(x) = K_1$ For $\Delta x < x \leq 2\Delta x,$where K_0 and K_1 are samples from the prescribed pdf.

I assume, for simplicity, that the values of K are uniformly distributed between the minimum and maximum values. If I further assume that erosion and isostatic rock uplift are both uniform and approximately in balance, then equation 4 can then be integrated to give

$$h(x) = \int_o^x \frac{E}{A^{1/2}\, K(X')}\, dx' , \qquad (5)$$

where$E$ is a constant. The model leading to equation 5 is based solely on the stream-power model for bedrock channel erosion. Channels in the Pachmarhi, however, are of mixed type, including both bedrock and alluvial reaches. Bedrock reaches in the Pachmarhi have a range of slopes from 0.1 (10%) to vertical, while alluvial reaches have lower slopes of between 0.05 and 0.07 (5%−7%). In order to include the effects of local alluvial storage in the model, we took the output of the stream-power model from equation 5 and backfilled all reaches where the slope was below $S_{min,}$ a prescribed minimum value for alluvial storage.

The resulting model is defined by five parameters: the ratio $E/A^{1/2}$ which has units of one over time, $K_{\min}$ and $K_{\max}$,, which also have units of one' over time, Δx which has units of length, and $S_{\min,}$ which is dimensionless.

Figures 12 and 13 illustrate the results of the model for different values of the input parameters, along with comparisons of the model to actual profiles in the Pachmarhi. Figure 12A plots the values of K obtained from sampling a uniform distribution between a minimum value $K_{\min} = 0.01Ka^{-1}$and a maximum value $K_{\max} = 1Ka^{-1}$usinga horizontal step size of $\Delta x = 10$m. The form of equation 5 indicates that the local channel slope is controlled by the inverse of K, not by K, so in Figure 12B we plotted K^{-1} for the same values of K shown in Figure 12A. When the values of $K^{-1}$are plotted, it is clear that, even though the values of K have a simple (uniform) distribution, the values of K^{-1}have a skewed distribution capable of producing values of K^{-1}that are much larger than its mean value. It is these extreme values of K^{-1} that cause the channel to hang locally and form structurally controlled knickpoints. Figure 12D plots the results of the model assuming $E/A^{1/2}$ = 0.02 ka^{-1}. In the limit where$K_{\min}$equals$K_{\max}$, the model predicts achannel segment of constant slope given by $s = E/(A^{1\backslash 2}K)$. As the difference between $K_{\min}$ and $K_{\max}$ increases in the model, the variability in longitudinal profile form and local slope also increases and the profiles become more stepwise. The model reproduces all of the qualitative features observed in the channels of the Pachmarhi, including steep, bedrock-dominated reaches characterized by a wide range of step sizes, alternating with gently sloping reaches with alluvial storage. For comparison, Figure 12C illustrates the longitudinal profiles of all channels >10 km in length draining the Pachmarhi. Alternating reaches of convexity and concavity and a stepwise character over a range of spatial scales is a universal characteristic of these channels. Equation 5 states that the channel longitudinal profile is the integral of random function. The simplest example of such a function is the random walk. In a simple random walk, the elevation can increase or decrease with equal probability by a prescribed amount Ah for each horizontal incrementΔh. Because the probability of an increase or decrease in elevation is equal for each horizontal increment, the average elevation of the random walk is always zero. Due to the probabilistic nature of the model, however, the random walk will exhibit excursions from its mean value. In the stream-power model with spatially random erodibility, mega- kickpoint zones (and their complement, the intervening reaches with alluvial storage) are the equivalent of the excursions of a random walk. Conceptually, mega-kickpoint zones form in the model when the cumulative bedrock erodibility falls below the mean value, which causes the channel to locally steepen above the mean channel slope. Conversely, when the cumulative bedrock erodibility is higher than average, the channel decreases in slope and becomes locally concave.

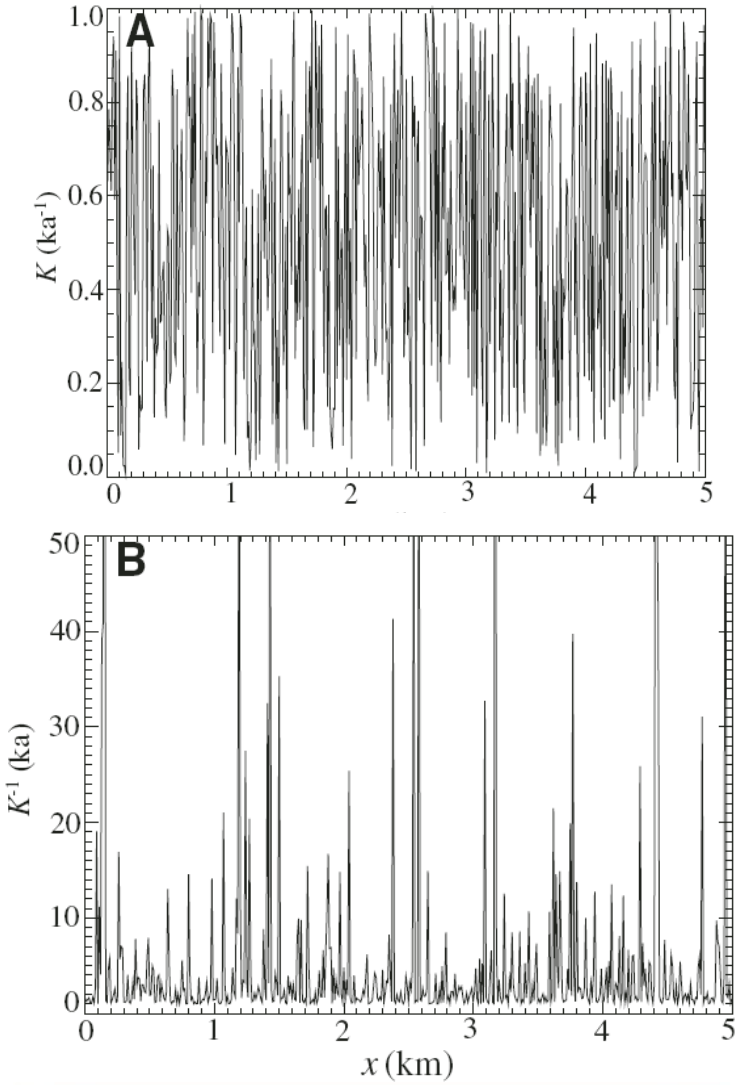
A
B
K (ka-1)
K-1 (ka)
x (km)
C
1
2
3
4
5
6
1.Dhupgarh 2. Balkandhar 3.Guttdeo 4. Phasi
5.Sonbhadra riftvalley 6.Denwa riftvalley

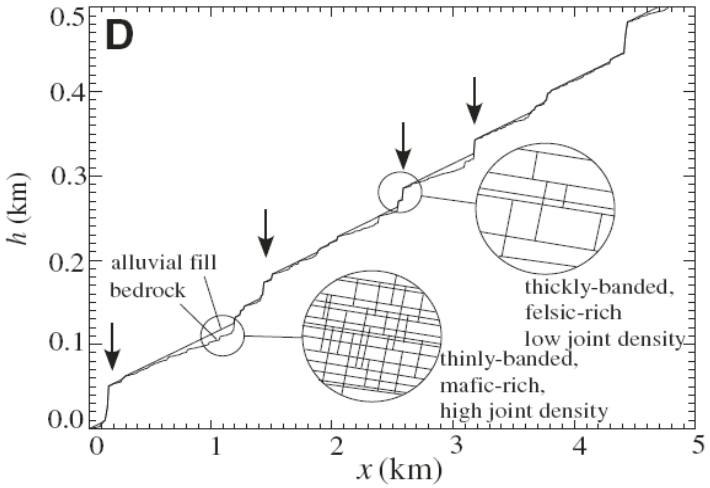

Figure: 12. Illustration of the components and results of the two-dimensional stochastic stream-power model for longitudinal profiles in the Pachmarhis. (A) Plot of bedrock erodibility*K*as a function of *x*, the distance along the channel profile, assuming Δx = 10 m, K_{min} = 0.01 ka^{-1} and K_{max} = 1 ka^{-1}. (See text for definitions.) (B) Plot of K^{-1} as a function of x. (C) Plots of the longitudinal profiles of majorheight and channels draining the Pachmarhi mountain(extract from the toposheets)(D) Plot of the longitudinal profile predicted by the model for the *K* values plotted in A and assuming $E/A^{1/2}$ = 0.02 ka^{-1} and 5_{min} = 0.07. Both the raw bedrock profile and the profile with alluvial backfilling are shown. The plot in D also illustrates the conceptual model schematically. In this conceptual model, areas of low *K* are associated with areas of low joint density, which, in turn, tend to be associated with unusually thick leucogranite sills. These zones tend to trigger knickpoint formation.

If the channel slope falls below the threshold $S_{\min,}$ alluvial backfilling occurs. The exact locations of these excur-minsions cannot be predicted, but their statistical properties can be predicted. A key goal of the modeling in this subsection is to predict the heights and spacings of the mega-kick point zones as a function of the model parameters, in order to better understand the controls on the geometry of structurally controlled longitudinal profiles in our study area and in similar areas with locally variable joint density.

If the probabilities of increase and decrease in a random walk are unequal, a linear trend will be superimposed on the random walk, causing the walk to trend up or down depending on which direction is favored probabilistically. In an analogous way, the elevation always decreases with increasing distance downstream in our model. To compute the average slope of the longitudinal profile predicted by the model, it is necessary to integrate the local slope over all possible values of *K,* weighted by the probability density function. This gives:

$$S_{av} = \frac{1}{(K_{max}-K_{min})}\frac{E}{A^{1/2}}\int_{K_{min}}^{K_{max}}\frac{dx}{x} = \frac{E}{A^{1/2}}\frac{\mathrm{In}K_{max}-\mathrm{In}\,K_{min}}{(K_{max}-K_{\max})} \quad (6)$$

Using the parameters chosen for the example given in Figure 12D, (6) gives $S_{av} = 0.093034$. This value is comparable to that of channel profiles in the Pachmarhi, which rise ~100 m for every 1 km of horizontal distance.

Several examples of the model output are presented in Figure 13B for the chosen parameters $\Delta x = 10\,m, K_{\min} = 0.01\,k^{-1}, K_{\max} = 1k^{-1}, E/A^{\frac{1}{2}} = 0.02\,k^{-1}$, and $S_{\min} = 0.07$. Actual longitudinal profiles from the Pachmarhi are plotted in Figure 13A for comparison. The profiles plotted in Figure 13B are each offset by 100 m so that they can be more easily distinguished in the figure. The stepwise character of the observed and modeled profiles can be highlighted by plotting a moving average (with a 200-m-wide window) of the slope of each profile (Figs. 13C, 13D). Note that the scale on the *y* axis of Figures 13C and

13D is divided sothat all of the plots can be shown on the same curve. Both the actual and the model profiles have mega-knickpoint zones (zones where the average slope exceeds 10% over length scales of 200 m) with typical spacings of ~0.5-1 km. The mega-kickpoint zones are not precisely periodic in the model or in nature, but they do have a characteristic distance between them that is approximately several hundred meters to 1 km.

The height of the largest knickpoint, h_{max}, in the model is controlled by the segment with the smallest value of the erodibility coefficient, K_{min}:

$$h_{max} = \frac{E\Delta x}{A^{1/2} K_{\min}} \tag{7}$$

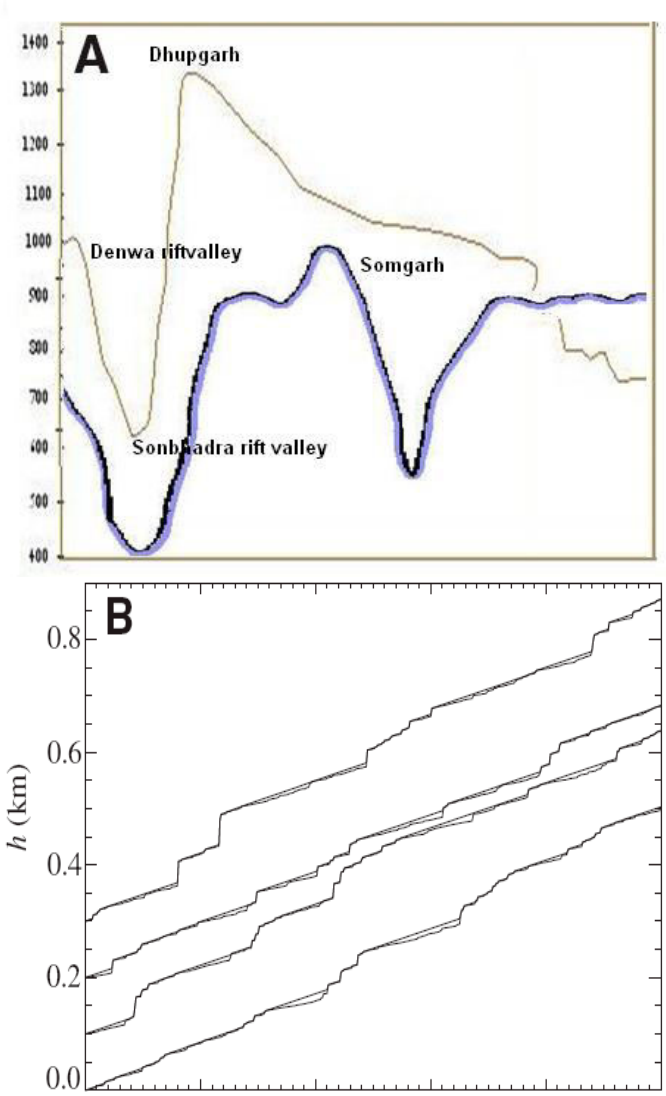

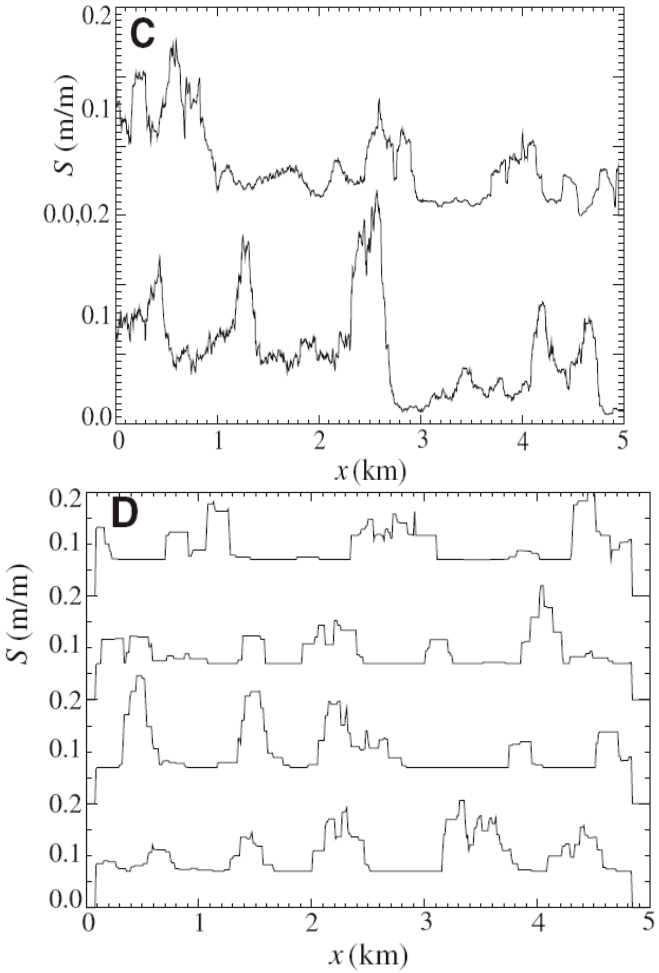

Figure: 13.Comparison of actual longitudinal profiles of Denwa and Sonbhadra along with Mountains with the model results. (A) Plots of the longitudinal profiles of Denwa and Sobhadra Canyons. (B) Plots of four example outputs of the model for Δx= 10 m, K_{min}= 0.01 ka^{-1}, K_{max} = 1 ka^{-1}, $E/A^{1/2}$ = 0.02 ka^{-1}, and S_{min} = 0.07. The profiles are offset by 100 m so that they are more easily distinguished. (C) Plot of the moving average of local channel gradient for the longitudinal profiles plotted in A. The moving average was computed using a window size of 200 m. Note that the scale on the *y* axis is divided so that both plots can be shown on the same curve. (D) Plot of the moving average of local channel gradient for the longitudinal profiles plotted in B. Both the actual and the model profiles have mega-knickpoint zones (zones, where the average slope exceeds 10% over length scales of 200 m) with typical spacings of ~0.5-1 km.

Using the parameters chosen for the example given in Figure 13, equation 7 gives h_{max}= 20 m. This value is larger than, but broadly consistent with, the largest knickpoints observed along in the Denwa and SonbhadraCanyon study sites, which are ~10 m in height. Equation 7 can also be used to calculate the height of every bedrock step in the model by replacing $K_{max}$with the local value of *K*. Figure 14 plots the cumulative distribution of bedrock step heights for Denwa and Sonbhadra canyonalong with the same distribution for the model (Fig. 14B). Both the real data and the model closely follow an exponential distribution (i.e., a straight line on log-linear scales) for large step sizes. At smaller step sizes, alluvial backfilling causes the steep spike in the model at low slopes because backfilling prevents any slopes lower than $S_{\min}$ from occurring. In the real data, alluvial backfilling occurs over a range of slopes rather than a single value, hence the spike at low slopes is more spread out compared to that in the model. It is difficult to compare the results of the model and the actual data with respect to the distribution of individual step heights precisely, because the model operates on

a 10 m horizontal scale (i.e., $\Delta x = 10$ m), while the DEM data have a resolution of 1 m. It is not possible to simply run the model at the same scale as the DEM resolution, however, because the value of Δx in the model is not just the resolution of the model output, it also represents the scale above which there is assumed to be no correlation in *K* values and below which *K* values are uniform. In the field, individual sills or light-toned bands exceed several meters in thickness, and field observations suggest that several thick sills can cluster together to form resistant rock units that can be as much as 10 m long laterally along the channel direction in the study area(Figure:14B). This observation suggests that $\Delta x = 10$ m is an appropriate value for the model, but it is difficult to be more precise. As a result of the difference in model and DEM resolutions, however, some ambiguity will necessarily exist in comparing the model predictions with DEM data with regard to individual step heights. That being said, it should be noted that step heights are the only measure of the model that depends on Ax. All of the other measures of longitudinal profile form we consider in this section (e.g., average slope, power spectrum, distribution of distances between mega-kickpoint zones) are independent ofΔx, and therefore may be directly compared readily with similar measures extracted from DEM data.

In order to compute the characteristic distance between mega-kickpoint zones predicted by the model, it is useful to introduce some additional concepts from the study of random walks. One of the fundamental properties of a random walk is that the root-mean-squared displacement of the walk increases with the square root of the horizontal distance, x. Specifically, the size of the average excursion of the walk is quantified using the root-mean-squared displacement, $\langle h^2 \rangle^{1/2}$ given by Gallager (1996) for any random walk as:

$$\langle h^2 \rangle^{1/2} = (S_{std} x)^{1/2}, \tag{8}$$

where the brackets denote an average value and $S_{std}$is the standard deviation of the slope at the scale of Δx.In the stream-power model with spatially random erodibility, S_{std}can be calculated as:

$$S_{std} = \frac{E}{A^{1/2}}\left(\frac{1}{K_{max}-K_{min}}\int_{K_{min}}^{K_{max}}\left(\frac{1}{x}-\left\langle\frac{1}{x}\right\rangle\right)^2 dx\right)^{1/2} = \frac{E}{A^{1/2}}\sqrt{-\left(\frac{In\,K_{max}-In\,K_{min}}{(K_{max}-K_{min})}\right)^2 - \frac{K_{max}^{-1}-K_{min}^{-1}}{K_{max}-K_{min}}}, \tag{9}$$

Using the parameters chosen for the example given in Figure 12D, equation 9) gives S_{std}= 0.220579. The average trend of the model above the minimum slope threshold set by $S_{\min}$is

$$h_{av} = (S_{av} - S_{min})x, \tag{10}$$

The characteristic spacing, λ_c, between mega-kickpoint zones is obtained by setting $\langle h^2 \rangle^{1/2}$ equal to h_{av} and solving for $x = \lambda_c$, At scales smaller than this characteristic distance, the random walk variations are, on average, greater than the linear trend in the model. At larger scales, the random walk variations are, on average, smaller than the linear trend. The characteristic spacing between mega-kickpoint zones coincides with the crossover between the random walk and deterministic linear trends, and is given by:

$$\lambda_c = \frac{S_{std}}{(S_{av}-S_{min})^2}, \tag{11}$$

Using the parameters chosen for the example given in Figure 12D, equation 11 gives λ_c, = 0.415 km.Predictions of the model can be compared in detail to the actual longitudinal profiles observed in the Pachmarhi in two principal ways. First, the power spectrum of a function quantifies the relative variability of that function at multiple scales. For a simple

random walk, the power spectrum is a power-law function of wave number, k, with an exponent of -2:

$$S(k) \propto k^{-2}, \tag{12}$$

A

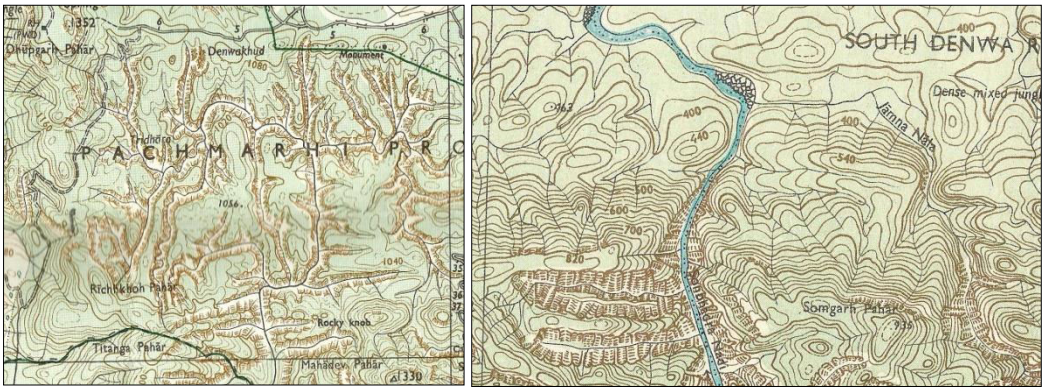

Denwa riftvalley **Sonbhadrariftvalley**

B

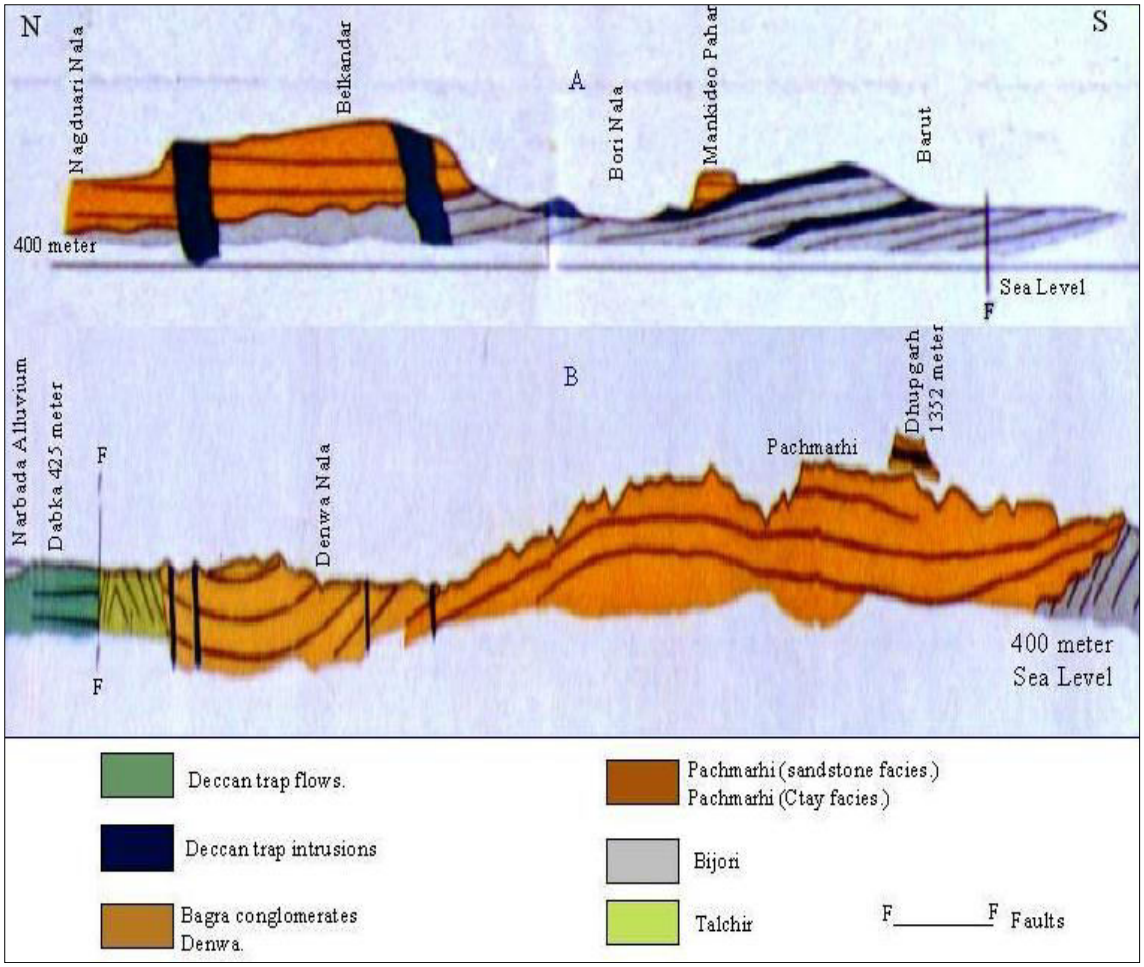

Figure: 14.Comparison of the cumulative distribution function of step heights. (A) Step heights observed in the toposheetsalong theDenwa and Sonbhadra rift valley at two stages in the elevation models. (B) Step heights in the model. In each case, the number of steps with a height greater than or equal to h is plotted as a function of h. Both distributions have an exponential form for large step heights. The distribution in B was obtained fromGeological map and toposheet.

Given the similarities between the stream-power model with spatially random erodibility and the simple random walk, it is reasonable to expect that the longitudinal profiles of the model and of the actual profiles observed in the Pachmarhi will also follow equation 12. The power spectrum is a powerful tool for analysis because, while random walk-like functions can look very different in the spatial domain, their power spectra all collapse to the same power-law dependence given by equation 12.

Figure 15A plots the power spectrum of the model along with the average power spectrum of the actual profiles of the Pachmarhi. In each case, the linear trend was first removed from both the model and actual data sets. Detrending is a standard preprocessing step in time series analysis and has the advantage that the power spectra will not depend on the magnitude of S_{av}, which varies depending on the model parameters. Figure.15Aplots the power spectra, $S(k)$, as a function of wave number, k, on logarithmic scales for the model (light gray curve, results obtained by averaging the spectra of 1000 independent simulations), for all of the channel profiles shown in Figure.12C , and for profiles of Denwa and Sonbhadra Canyons extracted from the toposheet. Also shown (straight black line) is the result for a simple random walk. The data sets and model closely follow the power spectrum of a simple random walk. This is not surprising considering that the model profiles (given by equation 5) are constructed from a model that is conceptually very similar to a random walk.

In addition to the power spectrum, the statistical distribution of distances between mega-kickpoint zones provides another basis of comparison for the model and actual profiles, as well as a means to test the model prediction for $\lambda_c$in equation 11. Equation 11 represents the characteristic distance between mega-kickpoint zones. Mega-kickpoint zones are not separated by a single value, but instead have a distribution of values. The distribution of distances between kickpoint zones can be calculated using the crossing statistics of a random walk. For a random walk, the distribution of intervals between successive crossings of the origin is given by a normalized exponential distribution (Gallager, 1996):

$$f(\lambda) = \lambda_{ce^{\dots\lambda/\lambda c}}\ , \tag{13}$$

where $\lambda_c$is given by equation 11. Figure.15B plots the normalized probability density function, $f(\lambda)$of the intervals between megaknickpoint zones for all of the channel profiles shown in Figure.12C .In order to compute the frequency distribution of distances between mega-kickpoint zones, it is necessary to define precisely mega-kickpoint for the purposes of the analysis. This definition is, to some extent, arbitrary because kickpoints have a range of sizes and distances between them. Nevertheless, we seek a definition of the mega-kickpoint zone that recognizes that kickpoints tend to come in clusters that are separated by zones of alluvial storage or backfilling.For the purposes of this analysis, we defined a mega-kickpoint zone in the model and in the real data to be any portion of the profile where the moving average of slope exceeds 0.15 or 15%. Using different definitions (i.e., smaller averaging windows and/or different thresholds for average slope) results in only slight differences in the results. For comparison, the light gray curve represents the exponential distribution (the expected distribution for a random walk process), i.e.,$f(\lambda) = \lambda_{ce^{-\lambda/\lambda c}}$, with $\lambda_c = 0.5$km. The exponential distribution clearly represents a good fit to the real and model data. The value of $\lambda_c$predicted by equation 11 should not be exactly equal to the value obtained by fitting the exponential distribution to the data in Figure 15B, because the analysis that led to the data included non-unique spatial averaging of the slope and a threshold criterion for the identification of mega-kickpoints. Nevertheless, the value of $\lambda_c$illustrated in Figure 15B (i.e., λ_c= 0.5 km)is in broad agreement with the theoretical value predicted by equation 11 (i.e., λ_c= 0.415 km).

The stream-power model with spatially random erodibility, despite its simplicity, is capable of reproducing the basic morphological features of channel longitudinal profiles in

the Pachmarhi. More broadly, the model provides a starting point for quantifying the structurally controlled complexity that exists in many bedrock (or mixed bedrock-alluvial) channel longitudinal profiles.

Structurally controlled kick-points are common in nature, but they have generally been underemphasized in bedrock erosion studies, partly because of the difficulty of incorporating structural information explicitly into numerical models. The stream-power model with spatially random erodibility provides one approach to including structural heterogeneity into landform evolution models, and it illustrates how small-scale structural heterogeneity can give rise to large-scale variations in longitudinal profile form.

Several caveats of the model should be noted. First, the model explicitly incorporates lateral variations in bedrock erodibility only. In nature, variations in erodibility will also be encountered vertically as channels incise. As such, a more realistic model would include both lateral and vertical variations in bedrock erodibility. Such a model would not achieve a static, steady-state geometry, but instead would reach a dynamic steady-state condition. Such a model would yield longitudinal profiles that exhibit random walk-like behaviour for snapshots in time, but knickpoints would shift laterally over time as new heterogeneities are exhumed. This point is particularly clear when considering the nature of alluvial storage in the model and in actual profiles. Zones of alluvial storage in eroding mountainand zones of alluvial storage through time. Second, the model assumes that banding is spatially uncorrelated below the resolution of the model (defined by the value of Δx). The fact that the power spectrum of the model matches the power spectrum of real topographic profiles from the Pachmarhi suggests that this assumption is correct to first order. However, no simple statistical model is likely to precisely honor the complexity of small-scale structural elements in real mountain belts. For example, leucogranite sills come in a variety of thicknesses, and field observations suggest that thick sills can occur in clusters. These complexities make it difficult to define a single, unique value for Δx.

Several additional caveats should be noted regarding the application of the stream-power model to channels of the Pachmarhi Mountains. First, the stream-power model is most accurately applied to channels undergoing plucking-dominated erosion.

Field evidence clearly indicates, however, that bedrock channels in the study area undergo both plucking-dominated and saltation-abrasion-dominated erosion, with the predominant process type depending on the local rock resistance to erosion (Figure:16). Modeling such process dependence on structure would require a more sophisticated model that includes stream-power-driven erosion, sediment-flux-driven erosion, and the transition between the two (e.g.,Gasparini et al., 2007). Structural kick-points may be enhanced as the dominant process switches from plucking to saltation abrasion within a structurally controlled knickpoint. The separation of flow from the channel bed may also enhance the persistence of kick-points (Crosby et al., 2007).

Also, channels respond to variations in rock type by varying both channel slope and channel width. Specifically, channels both narrow and steepen in response to more resistant rocks (Wohl and Merritt, 2001; Duvall et al., 2004; Amos and Burbank, 2007). Field evidence indicates that channels in the Pachmarhis respond similarly. The model of this paper does not explicitly vary the channel width in response to variations in rock strength or bedrock erodibility. This is an important limitation of the model that should be emphasized. It should also be noted, however, that bedrock erodibility coefficients in the model are empirical coefficients, which cannot (at this time) be calibrated directly based on quantitative measurements of joint spacing and/or rock hardness. Because K values areempirical, they can be defined to implicitly include the effects of channel width adjustment to variations in rock strength. In the absence of channel width variations, zones of unusually resistant bedrock would be characterized by even lower values of K than we assumed because the channel

would have to steepen even more that it already does in order to erode through those resistant units.

Therefore, by choosing an appropriate range of *K* values, the effects of channel width adjustment to variations in rock strength can be implicitly included so that the model predictions for variations in channel slope and longitudinal profile form are realistic.

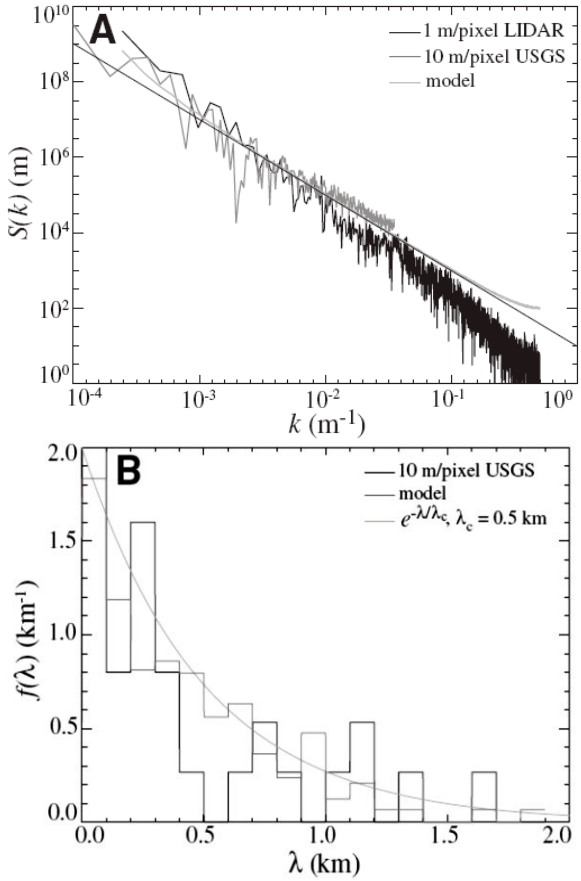

Figure: 15. Comparison of the results of the two-dimensional stochastic stream-power model for structurally controlled longitudinal profiles with the actual profiles of the Dhupgarh,-MahadevaandChauragarh mountains using power spectral analysis (A) and statistical analysis (B) of the distribution of intervals between mega-kickpoint zones. (A) Plot of the power spectrum, *S(k),* as a function of wave number, *k,* on logarithmic scales for the model (light gray curve, results obtained by averaging the spectra of 1000 independent simulations), for all of the channel profiles shown in Figure 12C. Profiles of Denwa and Sonbhadra Canyons extracted from the toposheets. Also shown (straight black line) is the result for a simple random walk. To first order, both the data sets and model closely follow the power spectrum of a simple random walk. (B) Plot of the normalized probability density function, $f(\lambda)$of the intervals between megaknickpoint zones for all of the channel profiles shown in Figure 12C and for the model. For comparison, the curves are represents the exponential distribution, i.e., $f(\lambda) = \lambda_{c e\lambda/\lambda c}$,with $\lambda_c = 0.5$km.

Conclusions

The Pachmarhis commonly exhibit drainages that are preferentially oriented parallel and perpendicular to the direction of tectonic extension. In this paper I have used field observations, DEM and aerial photographic analyses, and numerical modeling to test hypotheses for the structural and tectonic control of drainage architecture in the Pachmarhis. Field observations clearly show that channels preferentially exploit steeply dipping joint sets in the thePachmarhis. DEM analyses also show that drainage segments are more frequently

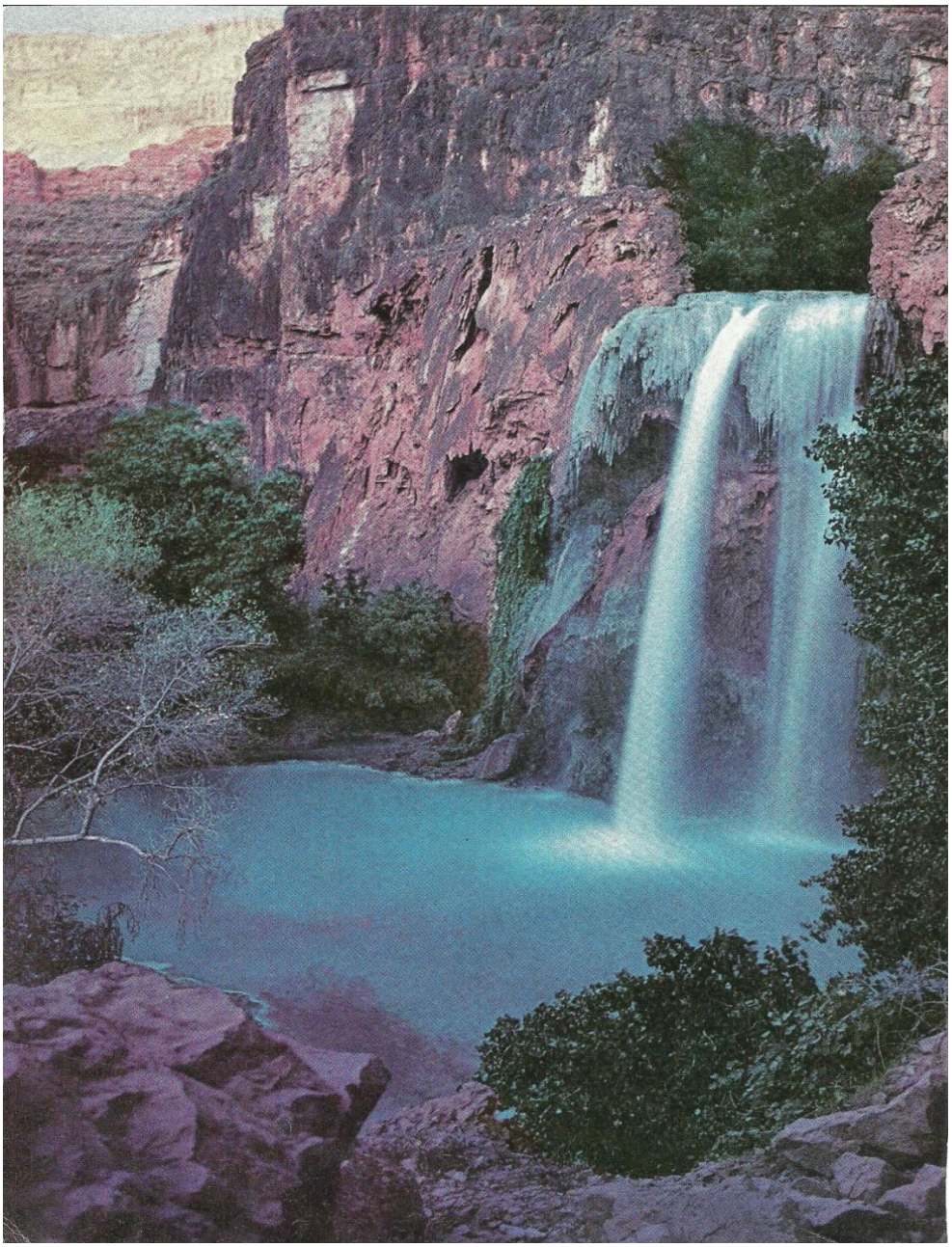

Figure:16 The waterfall on Jambudip River clearly indicates, however, that bedrock channels undergo both plucking-dominated and abrasion-dominated erosion, with the predominant process type depending on the local rock resistance to erosion

Oriented parallel to joint sets than along other directions. In order to test the joint-controlled hypothesis in more detail, we incorporated joint-controlled bedrock channel incision into a numerical model based on the stream-power model by using an orientation-dependent bedrock erodibility coefficient. The results of this numerical model indicate that joint-controlled bedrock channel incision alone is insufficient for producing the observed pattern of drainage architecture in the Pachmarhis. When an initial phase of extension-parallel tectonic tilting is also included in the model, the model predicts drainage architectures very similar to those observed.

Field observations indicate that structurally controlled kickpoints in the Pachmarhi are related to the exhumation of unusually thick, felsic-rich leucogranite sills with relatively

low joint densities. In order to better understand the relationship between spatial variations in joint density and variations in longitudinal profile form, I modified the numerical model using a spatially random bedrock erodibility coefficient. In topographic steady state, longitudinal profiles predicted by the model can be written as the integral of a random variable. The resulting model is similar to a random walk with a linear trend superimposed. The model illustrates how large-scale (1-10 km) steps in longitudinal profiles can develop from small-scale structural variations. As a stochastic model, the model cannot predict the exact configuration of structurally controlled kickpoints, but it can predict statistically the geometry of structurally controlled kickpoints and zones of alluvial storage. The model is capable of reproducing the basic features of longitudinal profiles of the Pachmarhi, including the power spectrum and the frequency-size distributions of bedrock steps and distances between mega-kickpoint zones. This model should form the basis for future studies that seek to quantify how spatial variations in bedrock erodibility influence longitudinal profile form.

References

Amos, C.B., and Burbank, D.W., (2007), Channel width response to differential uplift: Journal of Geophysical Research, v. 112,

Armstrong, R.L., (1982), Cordilleran The Pachmarhis—From Arizona to southern Canada: Annual Review of Earth and Planetary Sciences, v. 10, p. 129-154,

Attal, M., Tucker, G.E., Whittaker, A.C., Cowie, P.A., and Roberts, G.P., (2008), Modeling fluvial incision and transient landscape evolution: Influence of dynamic channel adjustment: Journal of Geophysical Research, v.

Bannister, E., (1980), Joint and drainage orientation of SW Pennsylvania: Zeitschrift fur Geo-morpho logie N.F., v. 24, p. 273-286.

Crookshank, H. (1936) Geology of the Nortern slopes of the Satpura between the morand and the sher river Memoirs, Geo , Sur IndVol LXVI Part.2

Crosby, B.T., Whipple, K.X., Gasparini, N.M., and Wobus, C.W., (2007), Formation of fluvial hanging valleys: Theory and simulation: Journal of Geophysical Research, v. ‘

Davis, G.H., and Coney, P.J., (1979), Geologic development of the Cordilleran The Pachmarhis: Geo logy, v. 7, p. 120-124,

Davis, G.H., Constenius, K.N., Dickinson, W.R., Rodriguez, E.P., and Cox, L.J., (2004), Faultand fault-rock characteristics associated with Cenozoic extension and core-complex evolution in the Catalina-Rincon region, southeastern Arizona: Geological Society of America Bulletin, v. 116, p. 128-141, doi: 10.1130/B25260.1.

Ehlen, J., and Wohl, E., (2002), Joints and landform evolution in bedrock canyons: Japanese Geomorp hological Union Transactions, v. 23, p. 237-255.

Eyles, N., Arnaud, E., Scheidegger, A.E., and Eyles, C.H., (1997), Bedrock jointing and geo-morphology in southwestern Ontario, Canada: An example of tectonic predesign: Geomorphology, v. 19, p. 17-34.

Finnegan, N.J., Roe, G., Montgomery, D.R., and Hallet, B., (2005), Controls on the channel width of rivers: Implications for modeling fluvial incision of bedrock: Geology,v. 33, p.

Fletcher, J.M., Bartley, J.M., Martin, M.W., Glazner, A.F., and Walker, J.D., (1995),Large-magnitude extension; An example from the central Mojave core complex: Geological Society of America Bulletin, v. 107, p.

Freeman, T.G., (1991), Calculating catchment area with divergent flow based on a regular grid: Compu ters & Geosciences, v. 17, p.

Gallager, R.G., (1996), Discrete stochastic processes: New York, Kluwer, 271 p.

Gasparini, N.M., Whipple, K.X., and Bras, R.L., (2007), Predictions of steady state and transient Land scape morphology using sediment-flux-dependent river incision models: Journal of Geophy sical Research, v. 112,

Hobbs, W.H., (1905), Examples of joint-controlled drainage from Wisconsin and New York: Journal of Geology, v. 13, p. 363-374.

Howard, A.D., (1994), A detachment-limited model of drainage-basin evolution: WaterResources Research, v. 30, p.

Miksa, E., (1993), Structural control of weathering on an exposed metamorphic core complex [M.S. thesis]: Tucson, University of Arizona, 31 p.

Miller, J.R., (1991), The influence of bedrock geology on knickpoint development and channel-bed

degradation along downcutting streams in south-central Indiana: Journal ofGeology, v. 99, p. 591-605.
Pain, C.F., (1985), Cordilleran The Pachmarhis in Arizona: A contribution from geomorphology: Geology, v.
Pazzaglia, F.J., Selverstone, J., Roy, M., Steffen, K., Newland-Pearce, S., Knipscher, W.,and Pearce, J., (2007), Geomorphic expression of midcrustal extension in convergentorogens: Tectonics, v.
Peterson, R.C., (1968), A structural study of the east end of the Pachmarhi, PimaCounty, Arizona [Ph.D. thesis]: Tucson, University of Arizona, 105 p.
Reynolds, S.J., (1982), Geology and geochronology of the South Mountains, central Arizona[Ph.D. thesis]: Tucson, University of Arizona, 220 p.
Richard, S.M., (1983), Structure and stratigraphy of the southern Little HarquahalaM ountains,La Paz County, Arizona [M.S. thesis]: Tucson, University of Arizona, 154 p.
Snyder, N.P., Whipple, K.X, Tucker, G.E., and Merritts, D.J., (2000), Landscape response to Tectonic forcing: Digital elevation model analysis of stream profiles in the Mendocino triple junc-*et al.*tion region, northern California: Geological Society of America Bulletin, v. 112, p. 1
Spencer, J.E., (1984), Role of tectonic denudation in warping and uplift of low-angle normalfaults: Geology, v. 12, p.
Spencer, J.E., (2000), Possible origin and significance of extension-parallel drainages in Arizona's The Pachmarhis: Geological Society of America Bulletin, v. 112,p.
Tarboton, D., (1997), A new method for the determination of flow directions and upslope areas in grid digital elevation models: Water Resources Research, v. 33, p.
Turowski, J.M., Lague, D., and Hovius, N., (2007), Cover effect in bedrock abrasion: A new derivation and its implications for the modeling of bedrock channel morphology:Journal of Geophysical Research, v.
Wagner, F.H., III, and Johnson, R.A., (2006), Coupled basin evolution and late-stage metamor-phic core complex exhumation in the southern Basin and Range Province, southeastern Arizona: Tectonophysics, v. 420, p.
Whipple, K.X, and Tucker, G.E., (1999), Dynamics of the stream power river incision model: Implica tions for height limits of mountain ranges, landscape response timescales and research needs: Journal of Geophysical Research, v.104, p.
Whipple, K.X, Hancock, G.S., andAnderson, R.S., (2000), River incision into bedrock: Mechanics and relative efficacy of plucking, abrasion and cavitation: Geological Society of America Bulletin, v. 112, p.
Whittaker, A.C., Cowie, P.A., Atal, M., Tucker, G.E., and Roberts, G.P., (2007), Bedrock channel adjustment to tectonic forcing: Implications for predicting river incision rates:Geology, v. 35, p. 103-106.
Willgoose, G., Bras, R.L., and Rodriguez-Iturbe, I., (1991), A coupled channel network growth and hillslope evolution model 1: Theory: Water Resources Research, v. 27, p.
Wobus, C.W., Crosby, B.T., and Whipple, K.X, (2006), Hanging valleys in fluvial systems: Controls on occurrence and implications for landscape evolution: Journal of Geophysical Research—Earth Surface, v. 111, no..
Wohl, E.E., (2008), The effect of bedrock jointing on the formation of straths in the Cache la Poudre \ River drainage, Colorado Front Range: Journal of Geophysical Research,v. 113, F01007, doi: 10.1029/2007JF000817.
Wohl, E.E., and Merritt, D.M., (2001), Bedrock channel morphology: Geological Society ofAmerica Bulletin, v.113, p.
Wohl, E.E., Thompson, D.M., and Miller, A.J., (1999), Canyons with undulating walls: Geological Soc i ety of America Bulletin, v. 111, p. 949-959,
Wust, S.L., (1986), Regional correlation of extension directions in Cordilleran metamorphic core Comp lexes: Geology, v. 14, p. 828-830,
Yin, A., (1991), Mechanisms for the formation of domal and basinal detachment faults: A three-Dimens ional analysis: Journal of Geophysical Research, v. 96, p.